OPERATION OF THE SUPARAMP AT 33 GHz*

R.Y. Chiao and P.T. Parrish

Department of Physics, University of California
Berkeley, California 94720

Received _____

ABSTRACT

A 9 mm degenerate parametric amplifier has been constructed using a linear, series array of unbiased Josephson junctions as the active, nonlinear element. We used a balanced diode mixer as a synchronous detector, with a single source serving both as the pump and as the mixer local oscillator. Stable, net gain of 15 dB in an instantaneous bandwidth (FWHM) of 3.4 GHz has been achieved. We measured a system noise temperature of 220 K ± 5 K (DSB) with a SUPARAMP contribution of only 20 K ± 10 K. Output saturation however has been observed. This complicates the interpretation of our noise temperature measurements and may render them upper limits. Comparison is made with the results of an earlier 3 cm SUPARAMP. The data are in substantial agreement with theoretical predictions.

*Work supported in part by NSF Grant AST 72-05136 and Nasa Grant NGL 05-003-272.

I. INTRODUCTION

In this article we report the successful operation of a 33 GHz parametric amplifier whose active element is a linear series-array of Josephson microbridges. We used both 80 and 160 junction arrays. The microbridges were integrated into a superconducting thin-film microstrip transmission line by a fabrication procedure to be described below. Together with a microstrip-to-waveguide transition and a three-port circulator, the system was operated as a reflection amplifier. We have named this device the SUPARAMP (Superconducting Unbiased Parametric Amplifier).

As in our previous work at 10 GHz[1,2] the amplifier was operated in the "doubly degenerate" mode with signal, pump and idler frequencies (ω_s,ω_p and ω_i, respectively) closely and equally spaced according to the relation

$$2\omega_p = \omega_s + \omega_i. \qquad (1)$$

However, in contrast to our previous work, the pump for the SUPARAMP and the local oscillator for the mixer following the SUPARAMP were derived from the same source in this experiment. This mode of operation, generally referred to as synchronous detection, automatically folds the amplified signal and idler channels into the same intermediate frequency channel. However, since the signal and idler channels are already intermixed as a consequence of the amplification process, synchronous detection does not then result in any loss of information. In fact, synchronous detection can result in an additional power gain of up to

6 dB compared with non-synchronous pumping, if an appropriate phase shift is introduced between the pump and the local oscillator.

II. EXPERIMENTAL

A. The microbridge array

The microbridge array was fabricated by an intersecting scratch technique described by Chiao et al[2]. Using a sharp diamond tool, a fine groove was scribed on a highly polished fused quartz substrate along the axis of what eventually was to become the upper conductor of the microstrip transmission line. A 1000 Å thin film of tin was then evaporated onto this substrate. The microstrip conductor pattern was photo-etched out of this film, with the groove coincident with the microstrip center line. Next, the substrate was scribed with the 80 or 160 lighter grooves perpendicular to the first, tin-filled groove. These lighter grooves removed the tin every-where along their paths except at the intersections with the deeper first groove. Thus a series of microbridges were formed. The typical dimensions of one of the microbridges, measured earlier from scanning electron microscope photographs,[3] are 1500 Å by 2500 Å wide. The junctions were regularly spaced 2.8 μm apart (for the 160 junction sample) or 5.6 μm apart (for the 80 junction sample) along the microstrip. These microbridge arrays are quite uniform and the fabrication yield for arrays (N ~ 100) is roughly 80%, with a high degree of reproducibility.[4] Figure 1 shows a portion of the string of the 160 microbridge sample used in this experiment.

The use of arrays simultaneously solves two important problems in the design of the SUPARAMP. The first problem is to optimally couple the active element to the external load.

The internal load of the amplifier arises from the shunt resistance of the microbridge, typically 1Ω. This is much smaller than the transmission line impedance $Z_0 \approx 50\Omega$. One of the design goals of the SUPARAMP is that the external load, the transmission line conductance, be larger than the internal load, the junction shunt conductance. With a linear, series of 100 microbridges in $Z_0 = 50\Omega$ microstrip, this requirement is simply met, without complicated or narrowband impedance matching. The second problem is saturation. The theory of the SUPARAMP[5] predicts from the depletion of pump photons by the amplification process that the maximum allowable thermal signal (or noise background) temperature before saturation sets in is

$$T_{sat}(K) = 1.4\ N^2\ \nu_{GHz}\ \Gamma_p^{-5/4}\ \frac{50}{Z_0}\ F \qquad (2)$$

where N is the number of junctions, ν_{GHz} is the frequency of operation in GHz, Γ_p is the peak gain of the amplifier, and F is a function of the coupling ($F = 1$ for $g \equiv NR_J/Z_0 >> 1$ and $F \approx 0.045\ g^{-5/2}$ for $g << 1$). For $\Gamma_p = 100$ (i.e. 20 dB gain), $F = 1$, $\nu_{GHz} = 33$, and $N = 1$, $T_{sat} = 0.14$ K. Thus the use of many junctions is required to obtain a practical saturation level.

B. The external circuitry and apparatus

We utilized an inverted microstrip[6] as the transmission line in these experiments. A microstrip 0.40 mm wide, supported by a 0.25 mm fused quartz substrate, was inverted and suspended 0.13 mm above a ground plane. This resulted in an impedance $Z_0 = 58\Omega$. In both the 80 and 160 junctions samples, the array spans distance $\lambda_g/17$ along the microstrip at 33 GHz,

thus ensuring that the microwave currents flow through each junction essentially in phase. The microstrip was terminated beyond the junctions by a $\lambda_g/4$ section of open circuited transmission line. This termination equivalently placed the junctions in shunt across the transmission line at 33 GHz and all odd harmonics. Immediately before the junctions, a tuning stub consisting of a $\lambda_g/12$ open-circuited transmission line was placed at a right angle. The purpose of this tuning stub is to short out third harmonic frequencies, the most important of which are the third harmonic of the pump ($3\omega_p$) and the undesirable upconversion products ($2\omega_p + \omega_s$ and $2\omega_p + \omega_i$). However because of a 50% error in the design of the $\lambda_g/12$ section, it is unlikely that these harmonics were effectively shorted.

A transition was made from the microstrip transmission line to the waveguide based on a design developed by Glance and Trambarulo.[7] The transition consisted of an extension of the microstrip center conductor into the waveguide, followed by a variable shorting plunger. Our transition yielded a return loss greater than 15 dB over an instantaneous bandwidth of 11%. The junction array with tuning stubs, the microstrip transmission line and the transition were housed as a single unit, which was located at the bottom of a 5 cm ID glass cryostat. The waveguide within the cryostat was slightly oversize (10.68 mm x 4.32 mm) with two tapered waveguide sections to standard size waveguide (7.11 mm x 3.56 mm) at each end, one at the microstrip transition and the other outside of the cryostat. The oversize

waveguide consisted of two sections. The first section, which passed through the top of the cryostat, was a 15 cm length of OFHC copper waveguide; the second was a 75 cm length of stainless steel waveguide 0.25 mm thick with a 7.5 μm gold plate on its inner surfaces. Loss measurements were made at 33 GHz both with the cryostat empty (at room temperature) and filled with liquid helium. The single pass losses were 0.88 dB and 0.36 dB respectively. In order to isolate the source and load, a three port waveguide circulator was employed outside the cryostat with an average isolation of 22 dB.

A schematic of the experiment is shown in Fig. 2. A single backward wave oscillator (BWO) is the common source of power for both the mixer local oscillator and the SUPARAMP pump. The pump power is derived from the BWO via two directional couplers and its amplitude can be adjusted by a precision attenuator. The local oscillator is derived from the same BWO and can independently be phase shifted as well as attenuated. The SUPARAMP is connected to port 2 of the circulator. Port 1 is connected to a matched load at either 295 K or 77 K depending on the state of switch A. The return loss from the two loads were 31 dB and 26 dB respectively. These data ensure that the loads are accurate thermal sources and that the standing wave ratio is small and very constant. In addition, a square-wave modulated noise tube, coupled by a 30 dB coupler, can add 11 K to

either input thermal source chosen. A filter following port 2 rejects second and third harmonics of the pump frequency by at least 35 dB. The output of the SUPARAMP exits through port 3 and is mixed down by a balanced mixer, using the synchronous local oscillator. The IF spectrum is amplified and displayed on a spectrum analyzer or measured by a total power detector.

III. RESULTS

A. The gain and noise measurements

Figure 3 shows the output of the total power detector as a function of pump power for the 160 junction sample at 2.9 K. The input to the SUPARAMP was the 77 K thermal load. The SUPARAMP can be removed from the system by placing switch B in the short position. This reference, the output for the mixer alone, with 77 K and 295 K signals is also displayed. The peak output with the SUPARAMP in the system increased only by 3% when the 77 K input was replaced by the 295 K input. A similar situation existed for the 80 junctions sample. This implies that the amplifier was either heavily saturated or noisy. To decide between these possibilities, we made similar measurements off the peak where a larger fractional change was observed and made noise measurements here. These noise measurements (described below) yielded a low noise temperature for the amplifier, thus supporting the saturation hypothesis. We point out that even on the steeper portions of the curve, the sensitivity of the output to changes in pump power are ΔP (output)/ΔP (pump) $\approx$ 0.1 dB/0.01 dB.

Differential gain and noise figure measurements were obtained using the 77 K thermal load and the noise tube. The noise tube was square wave chopped at 30 Hz, resulting in alternating 77 K and 88 K broadband radiation as the system input. The IF amplifier output was passed through

a 400-600 MHz filter and detected with a diode detector. The detected output was analyzed for its square wave component as well as its DC level. A system noise temperature, referred to switch A of 220 K ± 5 K was measured at a net differential gain of 15 dB. The effective input noise temperature excluding the mixer contribution, again referred to switch A, was calculated to be 110 K ± 10 K. By subtracting the noise contributions of the circulator and waveguide, the SUPARAMP noise temperature referred to the paramp mount was calculated to be 20 K ± 10 K. These noise temperatures are all double-sideband figures. Since the noise tube produces a small incremental change in the input temperature, the saturation level should not vary. The differential gain is then the most relevant figure when amplifying low level signals with a constant background of noise. However in light of the existence of saturation a determination of the noise temperature based on fluctuation measurements is more appropriate and may yield lower values.

B. The phase relationship between signal and idler

In order to verify the nature of the amplification process, the SUPARAMP was adjusted for high gain and measurements were taken of the total power output as a function of phase shift of the LO with respect to the pump. The dependence upon

this phase shift can be understood as follows. Let us define the voltage waveforms

$$V_k = v_k e^{j\theta_k} e^{j\omega_k t}$$

where k = p,s,i, LO and IF, stand for pump, signal, idler, local oscillator and intermediate frequency waves. According to the theory of the SUPARAMP the following phase relationship[5,8,9] exists between pump, signal and idler waves

$$2\theta_p = \theta_s + \theta_i + \frac{\pi}{2} - \Delta$$

For the degenerate case,

$$\Delta = \tan^{-1}[J_0(\alpha_p) - b_T g\xi]/[(1+g)\xi]$$

$$\xrightarrow[\text{gain}]{\text{high}} -\cos^{-1}[\xi(1+g)/|J_2(\alpha_p)|] \qquad (3)$$

where $\alpha_p = 2ev_p/\hbar\omega_p$, $\xi = \hbar\omega_p/2eI_JR_J$, and $b_T = -jY_TZ_o = +1/\sqrt{3}$ for our stripline circuitry. Here I_J is the critical current and Y_T the termination admittance. For $g<<1$, $\Delta = -14°$ and for $g>>1$, $\Delta = -20°$[8]. Neglecting any dispersion in the propagation between the SUPARAMP and the mixer by letting $\omega_s \rightarrow \omega_p \leftarrow \omega_i$ we can refer these phases to the spatial location of the mixer diodes. The resultant IF signal is then

$$V_{IF} \propto V_{LO}^{*} V_s + V_{LO} V_i^{*} + \text{c.c.}$$

$$\propto \cos(\theta_{LO} - \theta_p + \frac{\pi}{4} - \frac{\Delta}{2})\, e^{j(\omega_{IF}t + \theta_{IF})} + \text{c.c.} \qquad (4)$$

where we have made the approximations that $P_{LO} >> P_p$ and that at high gain $v_s = v_i$. Thus there is an interference between the IF produced by the signal and that produced by the idler. The phase of this interference is governed by the phase difference between the LO and the pump, with constructive interference occurring when

$$\theta_p - \theta_{LO} = \frac{\pi}{4} - \frac{\Delta}{2} + \pi n, \; n = 0, \pm 1, \pm 2, \ldots \qquad (5)$$

At these maxima the IF power output is a factor of four (i.e. 6 dB) larger than for that produced by the signal alone in a non-synchronous mode of detection[10] (i.e. where the LO frequency is not equal to the pump frequency). Figure 4 depicts the results of our measurements for the 80 junction sample. A cosine curve was fit to the data with amplitude and phase as free parameters. The light lines represent the detected outputs from 77 K and 295 K inputs without the SUPARAMP in the system. The dashed line represents the extrapolated detected output for zero K input entering port 2 of the circulator. If there were perfect destructive interference, the minimum of the cosine curve would coincide with this last line. However, the null is not quite perfect, implying a ratio of idler power to signal power ≤ 1.6.

C. The bandwidth

In order to measure the instantaneous bandwidth of the SUPARAMP, a spectrum analyzer was used to display the output IF spectrum from 0 to 1800 MHz of the 160 junction array.

The upper and lower traces in Fig. 5 represent the output with and without the SUPARAMP, respectively. The input in both cases was the 77 K thermal signal. In this case the shorting plunger behind the waveguide-to-microstrip transition was placed 2.0 mm away from the microstrip center line. Separately, the mixer noise temperature was measured to be 3250 K. If the average difference between the two traces is taken to be 3 dB, the SUPARAMP assumed noise free, would be operating with approximately 17 dB net gain. The 3 dB roll off point in Fig. 5 is approximately 1700 MHz. The bandwidth (FWHM) is twice this or 3.4 GHz. However this is actually a lower limit set by components external to the SUPARAMP. By mechanically returning the waveguide-to-microstrip transition from outside the cryostat to a position of 3.3 mm a narrow-band high gain mode could be obtained. This mode was characterized by 38 dB maximum gain and 4 MHz (FWHM) bandwidth. Retuning the shorting plunger to a position of 6.4 mm resulted in a narrow-band gain peak centered at a non-zero frequency. Both the amplitude and the frequency of the peak were a smooth function of the pump power as shown in Fig. 6.

IV. COMPARISON OF THEORY WITH EXPERIMENT

A theoretical analysis of the SUPARAMP has been published[5] and it is instructive to discuss the present results within the framework of that theory. The theory contains five physical parameters. The first three, the junction critical current I_J, the normal state resistance R_J and the number of junctions N, pertain to the active element, the microbridge array. The last two, the transmission line impedance Z_0 and the termination impedance Z_T, pertain to the passive circuitry. The theory predicts that the pump power at peak gain is $P \approx \frac{1}{8} I_J^2 Z_0$. From Fig. 3, $P = 5.0 \times 10^{-8}$ watts and it follows that $I_J = 80\ \mu A$. The theoretical gain-powerwidth product is $\Gamma_p^{3/4}(\Delta P/P) = 1.9$ in the limit $g>>1$, independent of the level of saturation. Therefore the experimental value of 2.0 ± 0.1 from Fig. 3 implies $g>>1$. The gain-bandwidth product $\Gamma_p^{1/2}(\Delta\nu/\nu) \geq 0.4$ is limited by the bandwidth of components external to the SUPARAMP and is consistent with $g>>1$. For $g>>1$ the theory predicts that the product $g\xi$ approaches a constant, 0.38. This allows us to further calculate the number of junctions N and their individual resistance R_J. Numerically we find $N = 26$ and $R_J = 2.2\ g$ ohms. The value of $I_J = 80\ \mu A$ is approximately 30% less than that determined in the 10 GHz experiment, and considerably less than the critical current measured for I-V characteristics of typical single junctions.[5] The value N = 26 indicates that not all of the junctions are participating in the amplification process, as was also found in the 10 GHz experiments. The individual junction resistance

R_J is expected to be of the order of an ohm, as determined from I-V characteristic measurements. This would seem to impose an upper limit of g of about unity, in contradiction to the conclusion based on the gain-powerwidth measurement. In the 10 GHz experiment values of g = 0.16 and R_J = 0.42 were deduced. At present these discrepancies are unresolved.

Another apparent discrepancy between experiment and theory is in the saturation level. The theoretical prediction from Eq. 2 is $T_{sat} = 1.6 \times 10^4$ K (N = 160, Γ_p = 15 dB, $Z_0 = 50\Omega$, g>>1). This value is two orders of magnitude greater than the saturation levels encountered in our experiments. However this discrepancy can be most probably explained by a combination of the following three effects:

(1) The gain Γ_p which appears in Eq. 2 is the unsaturated peak gain. The value of 15 dB used above was from a differential gain measurement <u>off</u> the peak. We expect the peak gain to be greater and the <u>unsaturated</u> peak gain to be greater still.

(2) Due to inhomogeneities in the array, not all junctions are expected to participate in the amplification process. This is consistent with the value N = 26 found in the previous paragraph, which would predict $T_{sat} = 4.2 \times 10^2$ K (the other parameters remaining constant).

(3) The error in tuning stub impedance results in a failure to short out the previously mentioned third harmonic frequencies. This error allows incident thermal radiation at the third harmonic frequency to be down converted to the

signal frequency and signal radiation to be unconverted and dissipated at the third harmonic. Both processes tend to lower the input saturation level.

From a comparison of Fig. 3 and a similar figure for the 80 junction sample (see also Fig. 4), the ratio of the maximum (saturated) noise rise for 160 to 80 junctions is 19. This is to be compared with the theoretical prediction of 4 (i.e. proportional to N^2), assuming Γ_p constant.

The extrapolated SUPARAMP noise temperature 20 K ± 10 K is to be compared with the expected thermal contribution $T(\text{physical})/g \approx 0.2\ K$[11] and quantum noise contribution $h\nu/k_B \ln 2 = 2.3$ K. The above error estimate of the extrapolated noise is perhaps too small as it does not take into account the uncertainty in thermal emission of the waveguide within the cryostat or the coupling losses of the waveguide-to-microstrip transition.

V. SUMMARY AND CONCLUSIONS

An amplifier of 33 GHz radiation has been successfully constructed using unbiased superconducting microbridges as its active element. This SUPARAMP possesses the desirable characteristics of high gain, wide bandwidth, low noise, low pump power and simplicity of design. One undesirable characteristic which it possesses is its low saturation level. However, for certain applications, e.g. radio astronomy, where essentially constant, low-level signals are encountered, this is not a serious disadvantage. From our previous work at 10 GHz, there was some doubt as to whether operation of 33 GHz was possible, since the $I_J R_J$ product from these experiments was 50 μV, only 0.06 of what we would expect from the superconducting energy gap.[5] The successful operation of the SUPARAMP at 33 GHz has dispelled these doubts. Encouraged by these results, experiments at 115 GHz have been initiated. In general, a qualitative comparison with the theory is satisfactory. The quantitative prediction of the gain-powerwidth product has been verified experimentally. The gain-bandwidth product and noise temperature measurements are not inconsistent with the theory. There exists some unresolved problems with the indirectly inferred quantities N and R_J. Finally, more work needs to be done to account for the thermal saturation quantitatively.

VI. ACKNOWLEDGEMENTS

We would like to thank Dr. Marc Feldman for his help on the theory, Prof. W.J. Welch for many useful discussions and the loan of equipment, and Prof. A.C. Cheung for a critical reading of the manuscript.

REFERENCES

1. P.T. Parrish and R.Y. Chiao, Appl. Phys. Lett. 25, 627 (1974).

2. P.T. Parrish, Ph.D. thesis (University of California, 1975) (unpublished).

3. R.Y. Chiao, M.J. Feldman, H. Ohta, P.T. Parrish, Rev. de Phys. Appl. (Paris) 9, 183 (1974).

4. In fact the 20% failure rate was caused not by the intersecting scratch technique, but by pinholes in the thin film.

5. M.J. Feldman, P.T. Parrish, and R.Y. Chiao, J. Appl. Phys. 46, 4031 (1975).

6. M.V. Schneider, Bell System Tech. J. 48, 1421 (1969), M.V. Schneider, B. Glance, W.F. Bodtmann, ibid., 48, 1703 (1969).

7. B. Glance and R. Trambarulo, IEEE Transactions on Microwave Theory and Techniques 21, 117 (1973).

8. Including the cosϕ term by the parameter ζ (see Ref. 5).
$\Delta = \tan^{-1} [J_0(1+\zeta^2\xi^2)+\zeta\xi^2(1+g) - b_T g\xi]/[\xi(1+g)+\zeta b_T g\xi^2]$
The range of Δ is -19.37° to -19.91° from $g<<1$ to $g>>1$, for $\zeta = -1$ and $b_T = \frac{1}{\sqrt{3}}$.

9. M.J. Feldman, Ph.D. thesis (University of California, 1975) (unpublished).

10. In Ref. 5, the gain is computed as the single sideband gain. In order to compare with these experiments we should add 6 dB to the SSB gain.

11. This noise temperature can be derived as follows. The known thermal noise source is the shunt resistance of the junctions at a physical bath temperature, T_p. We can substitute for this known source a hypothetical noise source at the input, provided that the noise voltage at the junctions remains constant. This procedure determines the temperature of the hypothetical source required to yield the same noise output.

FIGURE CAPTIONS

Fig. 1 Reflection microscope photograph of a portion of the 160 junction array. The individual junctions, spaced by 2.8 μm, are not resolved in this picture.

Fig. 2 Schematic of the experiment. The SUPARAMP was operated in a doubly degenerate mode, with synchronous detection, i.e. the BWO serves simultaneously as pump and local oscillator.

Fig. 3 Detected IF amplifier output vs. pump power. Data was obtained from the 160 junction sample. The heavy line represents a fit to output data for a 77 K input with the SUPARAMP in the system. Light lines (a) and (b) are the outputs without the SUPARAMP with 77 K and 295 K inputs, respectively. The phase shift was adjusted for maximum output.

Fig. 4. Detected IF amplifier output vs. phase shift. The zero in phase shift was arbitrarily chosen to fit a cosine curve through the output data, which was obtained from the 80 junction sample. The heavy line represents this fit for a 77 K input with the SUPARAMP in the system. Light lines (a) and (b) are the outputs without the SUPARAMP with 77 K and 295 K inputs, respectively. Dashed line (c) represents the output extrapolated to zero K input entering port 2 of the circulator. The pump power was adjusted to give maximum output. The pump power drifted somewhat for data represented by

the open circles, and they should be taken as lower limits.

Fig. 5 Spectrum analyzer display of the IF spectrum. The vertical scale is 2 dB per division and the horizontal scale is 180 MHz per division. Data was obtained using the 160 junction sample. The upper trace represents the output for a 77 K input with the SUPARAMP in the system. The lower trace represents the output for a 77 K input without the SUPARAMP. The mixer noise temperature was 3900 K. The ripples in the upper trace are due to reflections between the circulator and the SUPARAMP mount.

Fig. 6 Spectrum analyzer display of a portion of the IF spectrum. The 160 junction sample was used. The vertical scale is 7 dB per division and the horizontial scale is 10 MHz per division, with 210 MHz at the center. Starting from the top trace the relative pump power level was (a) 0 dB, (b) +0.05 dB, (c) +0.1 dB, (d) +0.2 dB, and (e) +0.3 dB.

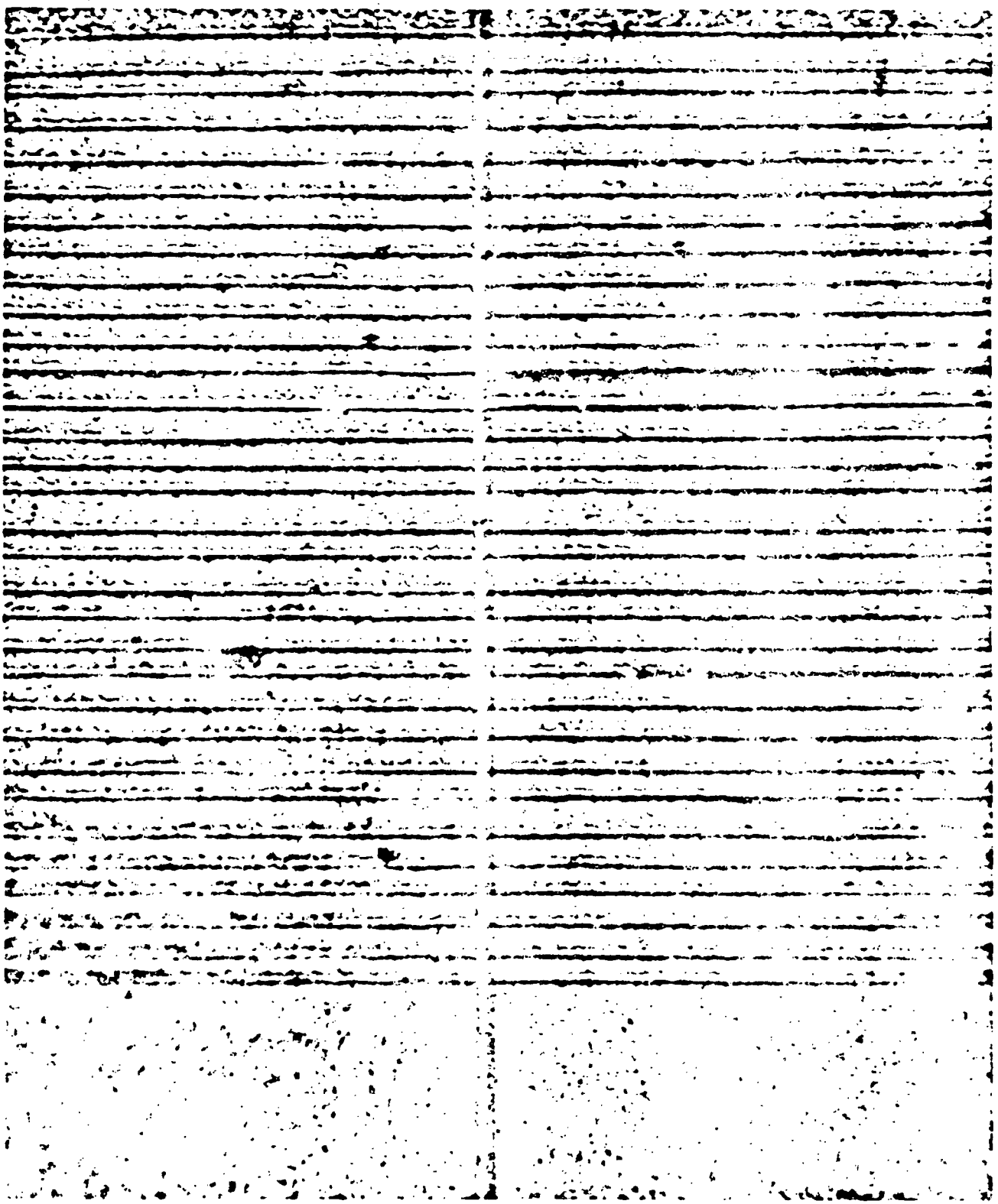

Fig. 1

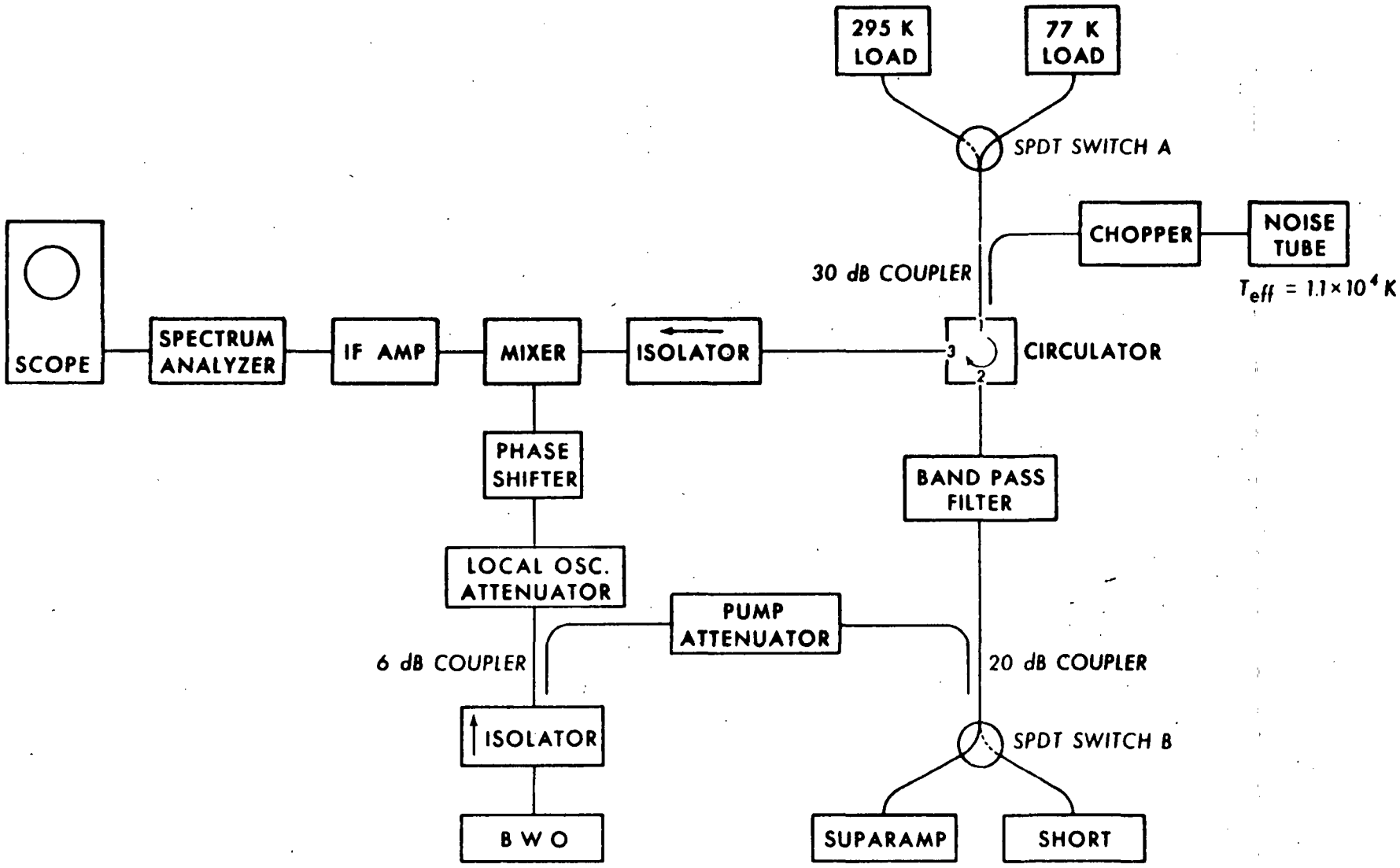
295 K LOAD
77 K LOAD
SPDT SWITCH A
CHOPPER
NOISE TUBE
T_{eff} = 1.1×10⁴ K
30 dB COUPLER
SCOPE
SPECTRUM ANALYZER
IF AMP
MIXER
ISOLATOR
3
2
CIRCULATOR
PHASE SHIFTER
BAND PASS FILTER
LOCAL OSC. ATTENUATOR
PUMP ATTENUATOR
6 dB COUPLER
20 dB COUPLER
ISOLATOR
SPDT SWITCH B
B W O
SUPARAMP
SHORT

Fig 2

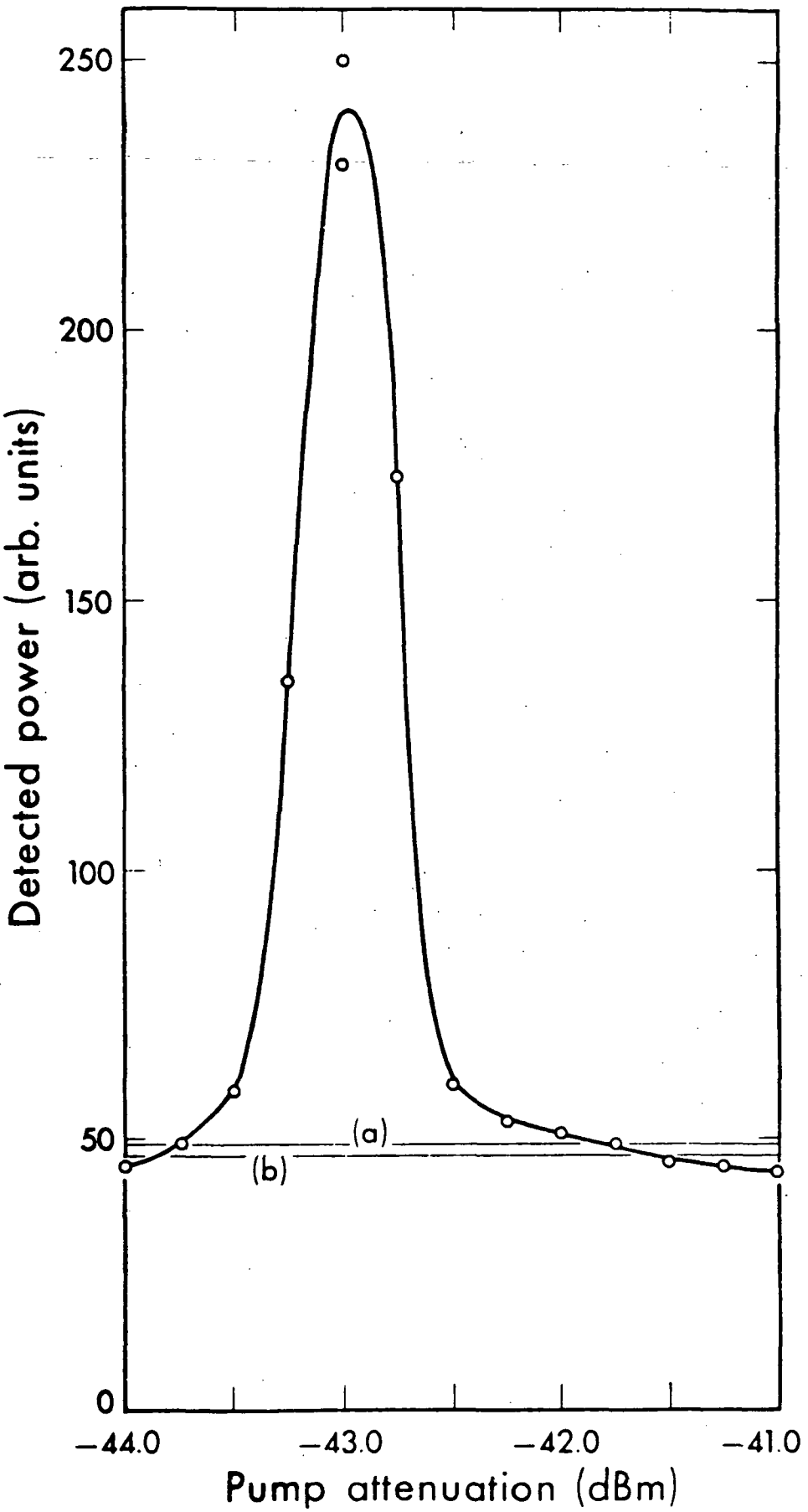
250
200
150
100
50
0
Detected power (arb. units)
(a)
(b)
−44.0
−43.0
−42.0
−41.0
Pump attenuation (dBm)

Fig. 3

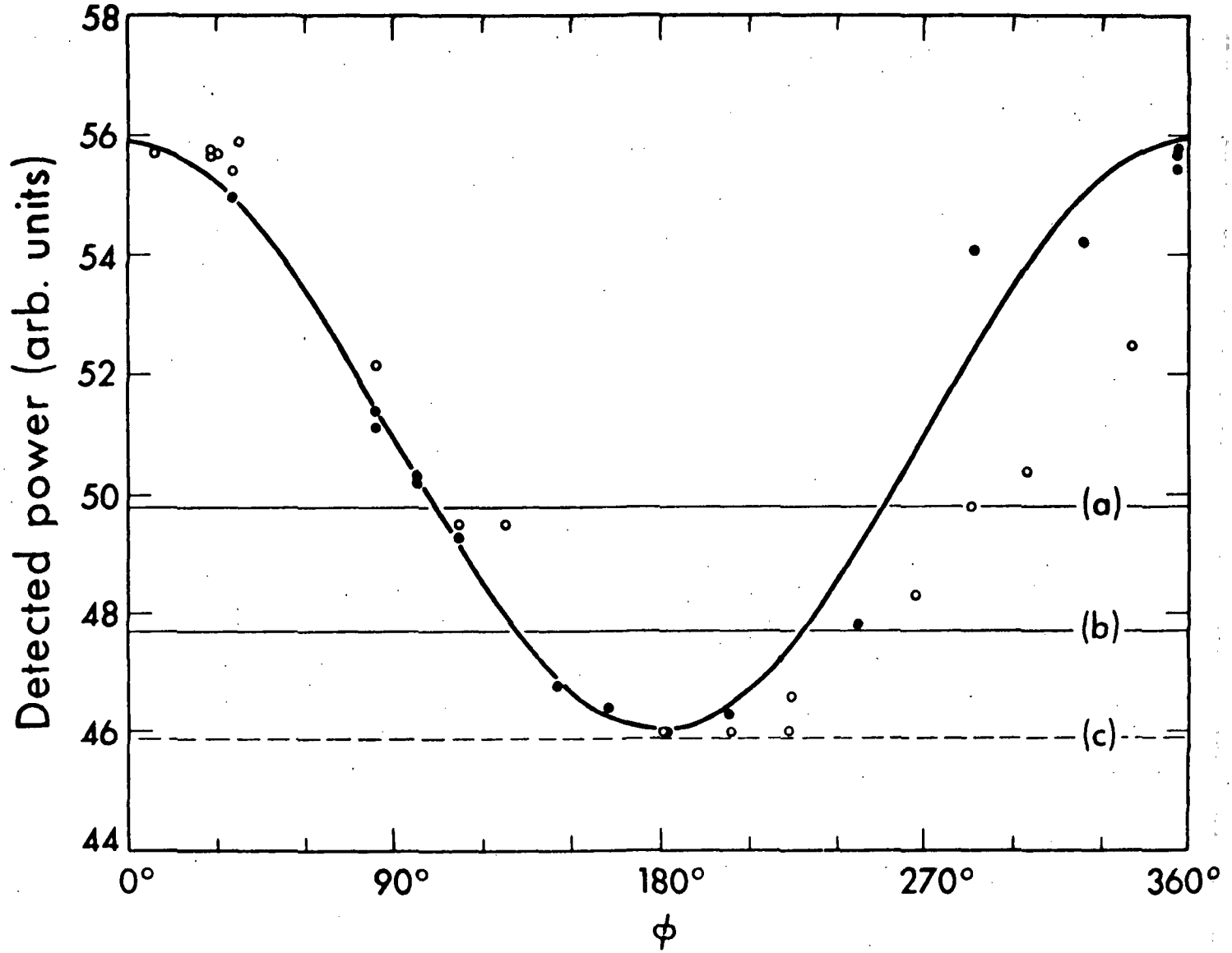
58
56
54
52
50
48
46
44
Detected power (arb. units)
(a)
(b)
(c)
0°
90°
180°
270°
360°
φ

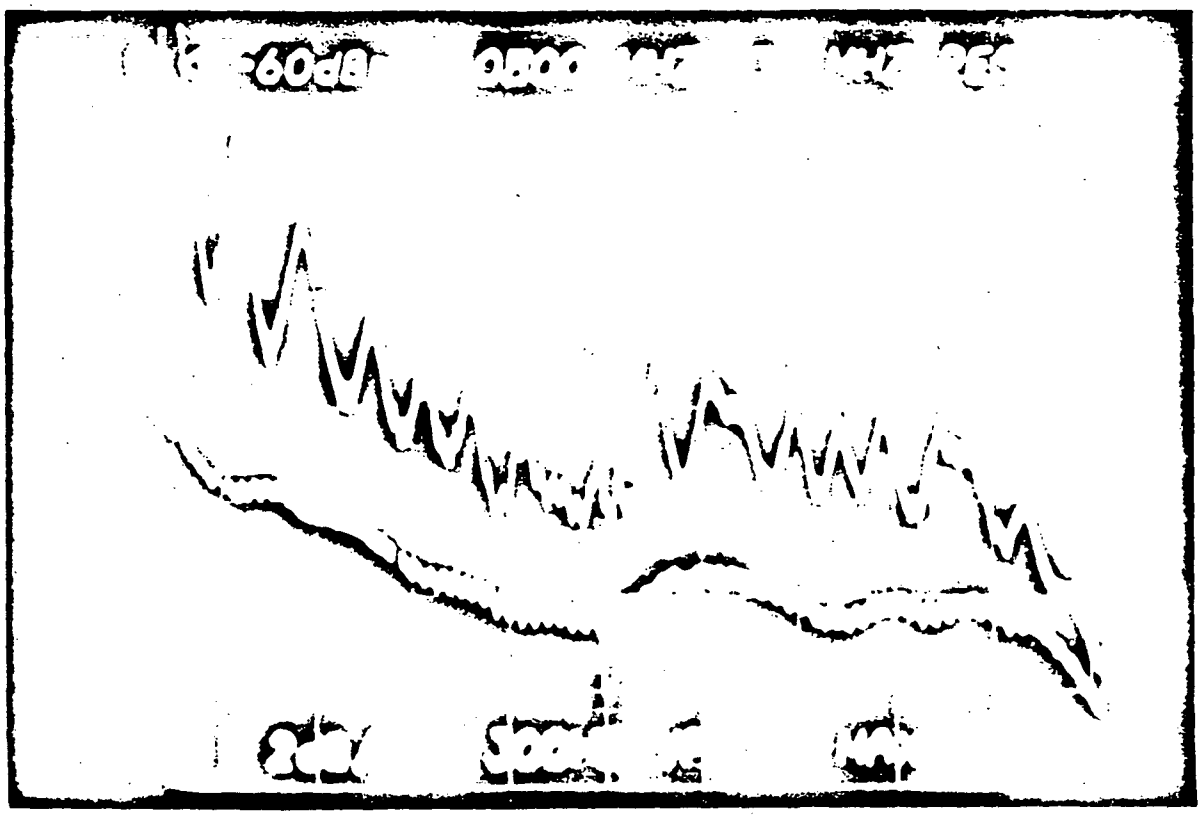

Fig. 5

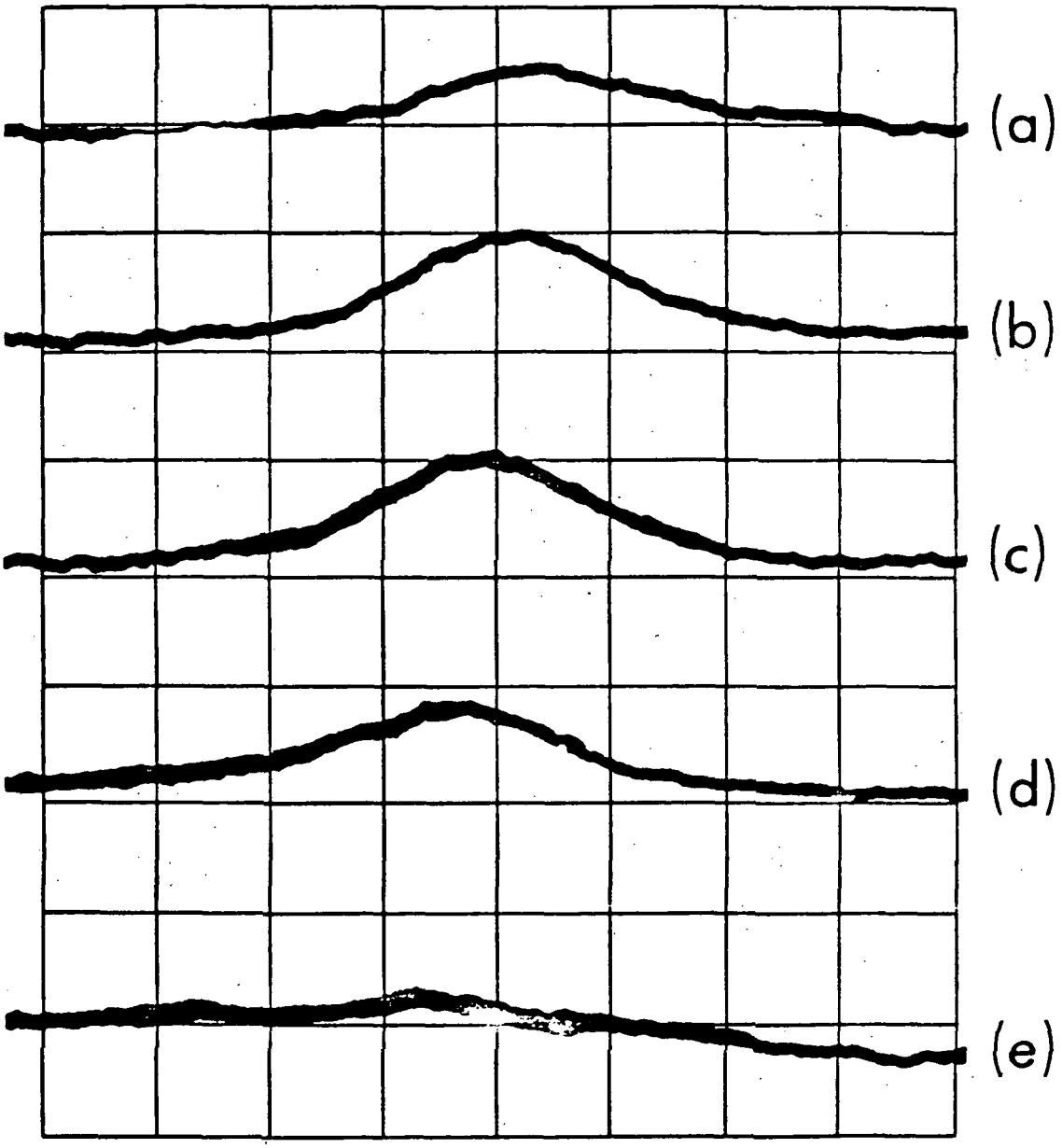

Fig. 6